Table VI. Atomic Coordinates (×10⁴) for 3 and Equivalent Isotropic Displacement Coefficients (Å² × 10³)

	x	y	z	U(eq)[a]
K(1)	3378 (1)	4396 (1)	3145 (1)	57 (1)
Zn(1)	3512 (1)	5868 (1)	4138 (1)	42 (1)
Si(1)	922 (1)	6313 (1)	1217 (1)	52 (1)
Si(2)	6145 (1)	6815 (1)	4075 (1)	54 (1)
Si(3)	2954 (1)	5560 (1)	7056 (1)	57 (1)
C(1)	2172 (4)	5696 (2)	2084 (3)	54 (2)
C(2)	1803 (6)	6923 (2)	634 (5)	98 (3)
C(3)	−642 (4)	6041 92)	−394 (4)	73 (2)
C(4)	144 (5)	6644 (2)	2423 (5)	92 (2)
C(1′)	4755 (4)	6614 (2)	4734 (4)	50 (2)
C(2′)	7980 (4)	6569 (2)	5319 (5)	86 (2)
C(3′)	6252 (6)	7641 (2)	3828 (6)	94 (3)
C(4′)	5824 (5)	6456 (2)	2333 (5)	84 (2)
C(1″)	3300 (4)	5247 (2)	5564 (3)	49 (1)
C(2″)	4672 (5)	5677 (2)	8641 (4)	85 (2)
C(3″)	1811 (7)	5065 (3)	7641 (6)	112 (4)
C(4″)	2053 (6)	6303 (2)	6592 (6)	98 (3)

[a] Equivalent isotropic U defined as one-third of the trace of the orthogonalized U_{ij} tensor.

Table VII. Atomic Coordinates (×10⁴) for 4 and Equivalent Isotropic Displacement Coefficients (Å² × 10³)

	x	y	z	U(eq)[a]
K(1)	4048 (1)	−247 (1)	11261 (2)	86 (2)
Zn(1)	4761	238	8622	65 (1)
Si(1)	4414 (1)	−940 (1)	7838 (3)	80 (2)
Si(2)	5255 (2)	1152 (2)	6910 (3)	112 (3)
C(1″)	4251 (4)	412 (4)	9276 (7)	52 (5)
C(2″)	3724 (4)	72 (4)	9202 (7)	66 (6)
C(3″)	3361 (4)	145 (5)	9740 (9)	89 (7)
C(4″)	3508 (6)	537 (5)	10411 (10)	98 (9)
C(5″)	4020 (6)	886 (5)	10481 (8)	85 (7)
C(6″)	4373 (4)	816 (4)	9920 (8)	66 (6)
C(1)	4574 (4)	−503 (4)	8938 (8)	80 (6)
C(1′)	5377 (3)	765 (4)	7800 (7)	71 (6)
C(2)	4996 (4)	−790 (5)	7118 (9)	142 (8)
C(3)	4140 (6)	−1619 (5)	8247 (14)	212 (10)
C(4)	3937 (5)	−927 (6)	6993 (10)	170 (10)
C(2′)	4709 (6)	775 (8)	6152 (14)	355 (12)
C(3′)	5080 (8)	1564 (8)	7599 (14)	335 (13)
C(4′)	5784 (5)	1560 (5)	6046 (10)	141 (9)
Sol(1)	3333	−3333	6667	300
Sol(2)	3333	−3333	1667	300
Sol(3)	3333	−3333	4947 (35)	300
Sol(4)	3333	−3333	147 (40)	300

[a] Equivalent isotropic U defined as one-third of the trace of the orthogonalized U_{ij} tensor.

°C dec; ^{1}H NMR δ 0.39 (s, Me), −0.94 (s, CH_2), 7.01, 7.17, 7.74 (m, Ph); $^{13}C\{^1H\}$ NMR 3.12 (br, CH_2), 4.32 (Me), 125.5, 127.7, 139.5 (Ph). Anal. Found (calcd) for $C_{14}H_{27}Si_2KZn$: C, 47.32 (47.23); H, 7.79 (7.64); K, 11.10 (10.98).

(c) Stirring potassium (0.108 g, 2.76 mmol) and $Zn(CH_2SiMe_3)_2$ (0.95 g, 3.96 mmol) under 1 atm of He in a Pyrex tube for 1 day resulted in a black coating on the potassium. The reaction became rapid as soon as the temperature was raised above the melting point of potassium, and the mixture was stirred for 20 min at 95 °C. The gray solid was mixed with benzene, the mixture was filtered, and the filtrate was reduced in vacuo to a yellow gum, which slowly crystallized. NMR spectroscopy showed **3** only.

Crystallographic Studies on 1–4. Suitable crystals were mounted in thin-walled glass capillaries. Data collection for all four structures utilized automated Siemens R3m/V diffractometers with incident-beam graphite monochromators. Mo Kα (λ = 0.710 73 Å) radiation was used for 1·C_6H_6 through **3** and Cu Kα (λ = 1.541 78 Å) radiation for **4**. Data were corrected for Lorentz and polarization effects, and semiempirical absorption corrections based on the ϕ dependence of 10–12 reflections with χ ca. 90° were applied. Maximum and mininum transmissions were 0.62 and 0.43, 0.98 and 0.80, 0.89 and 0.82, and 0.75 and 0.38, respectively, for 1·C_6H_6 through **4**. Space group determinations were based on extinctions present and confirmed by the structure solutions. In each case the structures were determined by direct methods and refined using full-matrix least-squares methods as implemented by the program SHELEXTL.[12] In all structures the parameters refined included the coordinates and anisotropic thermal parameters for all but the hydrogen atoms. Hydrogen atoms were placed in idealized positions (C–H = 0.96 Å), and the coordinate shifts for carbon were applied to the bonded hydrogens. In **2** and **3** methyls were treated as rigid groups and allowed to rotate. In all cases the isotropic thermal parameters for the hydrogens were fixed. In **4** the solvate is disordered and is present in only partial occupancy. No identification of the solvate could be made, and only electron density as a fraction of carbon on the $\bar{3}$ axis was included, although the space available could accommodate hexane or benzene. Additional data collection and refinement parameters are given in Table I. Thermal ellipsoid plots in Figures 1–4 are drawn at the 20% probability level.

Acknowledgment. We thank the ONR for financial support.

Registry No. 1·C_6H_6, 140411-47-8; **2**, 140411-48-9; **3**, 140411-49-0; **4**, 140411-50-3; $Zn(CH_2CMe_3)_3$, 54773-23-8; $Zn(CH_2SiMe_3)_2$, 41924-26-9.

Supplementary Material Available: Tables of bond lengths, bond angles, anisotropic displacement coefficients, and H atom coordinates for 1·C_6H_6, **2**, **3**, and **4** (16 pages). Ordering information is given on any current masthead page.

OM910792T

(12) Sheldrick, G. M. SHELEXTL80, An Integrated System for Solving, Refining, and Displaying Crystal Structures from Diffraction Data; University of Göttingen: Göttingen, Federal Republic of Germany, 1980.

Photoactivated Gas-Phase Ligand Switching

R. Marshall Pope and Steven W. Buckner*

Department of Chemistry, University of Arizona, Tucson, Arizona 85721

Received September 1, 1991

Summary: The photoinitiated ligand-switching reaction of $VC_6H_6^+$ with CH_3CN at 604 nm to generate VCH_3CN^+ is reported. Photodissociation measurements indicate the reaction proceeds on a single minimum potential surface with an endothermic activation barrier.

Condensed-phase ligand photosubstitution reactions have been examined in great detail.[1-4] The vast majority of these reactions proceed by dissociative mechanisms

(1) (a) Geoffroy, G. L.; Wrighton, M. S. *Organometallic Photochemistry*; Academic Press: New York, 1979. (b) Skibsted, L. H. *Coord. Chem. Rev.* **1989**, *94*, 151.
(2) Ford, P. C. *Coord. Chem. Rev.* **1982**, *44*, 61.
(3) Geoffroy, G. L. *J. Chem. Educ.* **1983**, *60*, 861.

0276-7333/92/2311-1959$03.00/0

which are initiated by photodissociation of a ligand to generate a coordinatively unsaturated complex (reaction 1). Many of these photochemical reactions have been found to have synthetic utility. Ligand photosubstitution reactions occurring by associative mechanisms, as in reaction 2, are much less prevalent.[4]

$$ML_2 + h\nu \rightarrow ML + L \xrightarrow{+L'} MLL' \quad (1)$$

$$ML_2 + h\nu \rightarrow [ML_2]^* + L' \rightarrow [ML_2L']^* \rightarrow MLL' + L \quad (2)$$

The photochemistry of gas-phase inorganic and organometallic complexes has been a topic of recent interest due to the development of methods for generating highly unsaturated and unusual gas-phase organometallic complexes.[5-8] These studies have focused almost exclusively on photodecomposition pathways and photodissociation spectra.[6-9] There have been only two reports on the bimolecular photochemistry of inorganic complexes in the gas phase,[10] including photoinduced rhodocene formation ($Rh(c\text{-}C_5H_5)_2^+$) and photoenhanced oxidation of Co_2NO^+. This is consistent with the paucity of photochemically driven bimolecular reactions under low-pressure gas-phase conditions.[11] The photochemistry of $V(C_6H_6)_n^+$ complexes (n = 1, 2) in the gas phase is reported here, including the first observations of gas-phase photoinduced ligand substitution.

Experimental Section

All experiments are performed on a Fourier transform ion cyclotron resonance mass spectrometer.[12,13] The trapping cell is a single chamber with dimensions 2.75 × 1.375 × 1.375 in. The excite plates have been replaced with tungsten screens (transmittance >80%) to allow photoexcitation of ions trapped in the cell. The magnetic field is supplied by a Varian electromagnet regulated at ~0.7 T. The trapping cell and experimental pulse sequences are controlled by a Nicolet FTMS-2000 computer.

Scheme I

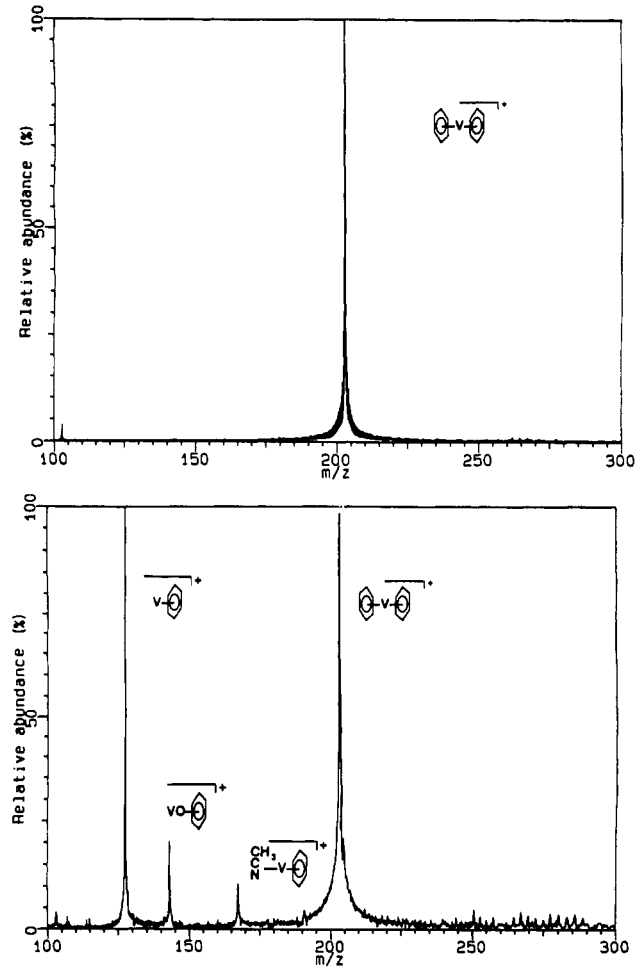

Figure 1. Mass spectra of $V(C_6H_6)_2^+$ trapped for 3 s in 2×10^{-6} Torr CH_3CN: (a, top) without laser irradiation; (b, bottom) with irradiation from an Ar^+ laser (~3 W all lines). The peak at m/e 145 corresponds to $V(C_6H_6)O^+$ generated by reaction of $V(C_6H_6)^+$ with background O_2.

V^+ is generated by desorption/ionization from a pure vanadium rod using the focused fundamental (1064 nm) output from a Spectra-Physics DCR-11 pulsed Nd:YAG laser with pulse energies on the order of 95 mJ/pulse.[15] The laser and mass spectrometer are synchronized using a home-built laser interface.[16]

Cyclohexene reacts with V^+ via two successive hydrogen eliminations to generate the metal ion–benzene complexes, as in reactions 3 and 4. Cyclohexene is admitted into the cell through

$$V^+ + c\text{-}C_6H_{10} \rightarrow V(C_6H_6)^+ + 2H_2 \quad (3)$$

$$V(C_6H_6)^+ + c\text{-}C_6H_{10} \rightarrow V(C_6H_6)_2^+ + 2H_2 \quad (4)$$

a General Valve Corp. Series 9 pulsed valve driven by a home-built pulsing circuit. The gas pressure wave emitted from the pulse valve reaches a maximum pressure of ~5×10^{-5} Torr and is

(4) (a) Monsted, L.; Monsted, O. *Coord. Chem. Rev.* **1989**, *94*, 109. (b) Hollebone, B. R.; Langford, C. H.; Serpone, N. *Coord. Chem. Rev.* **1981**, *39*, 181. (c) Fukuda, R.; Walters, R. T.; Adamson, A. W. *J. Phys. Chem.* **1979**, *83*, 2097.

(5) (a) Allison, J. *Prog. Inorg. Chem.* **1986**, *34*, 628. (b) *Gas Phase Inorganic Chemistry*; Russell, D. H., Ed.; Plenum Press: New York, 1989.

(6) Dunbar, R. C. Chapter 10 in ref 5b.

(7) (a) Hettich, R. L.; Jackson, T. C.; Stanko, E. M.; Freiser, B. S. *J. Am. Chem. Soc.* **1986**, *108*, 5086. (b) Hettich, R. L.; Freiser, B. S. *J. Am. Chem. Soc.* **1986**, *108*, 2537. (c) Hettich, R. L.; Freiser, B. S. *J. Am. Chem. Soc.* **1987**, *109*, 3543. (d) Cassady, C. J.; Freiser, B. S. *J. Am. Chem. Soc.* **1984**, *106*, 6176.

(8) (a) Tecklenberg, R. E.; Russell, D. H. *J. Am. Chem. Soc.* **1987**, *109*, 7654. (b) Tecklenberg, R. E.; Bricker, D. L.; Russell, D. H. *Organometallics* **1988**, *7*, 2506.

(9) (a) Dunbar, R. C.; Hutchinson, B. B. *J. Am. Chem. Soc.* **1974**, *96*, 3816. (b) Richardson, J. H.; Stephenson, L. M.; Brauman, J. I. *J. Am. Chem. Soc.* **1974**, *96*, 3671. (c) Rynard, C. M.; Brauman, J. I. *Inorg. Chem.* **1980**, *19*, 3544. (d) Engelking, P. C.; Lineberger, W. C. *J. Am. Chem. Soc.* **1979**, *101*, 5569. (e) Hanratty, M. H.; Paulsen, C. M.; Beauchamp, J. L. *J. Am. Chem. Soc.* **1985**, *107*, 5074.

(10) (a) Gord, J. R.; Buckner, S. W.; Freiser, B. S. *J. Am. Chem. Soc.* **1989**, *111*, 3753. (b) Gord, J. R.; Freiser, B. S. *J. Am. Chem. Soc.* **1989**, *111*, 3754.

(11) The only other report of a gas-phase photoinduced bimolecular ion–molecule reaction may be found in: Bomse, D. S.; Beauchamp, J. L. *J. Am. Chem. Soc.* **1980**, *102*, 3967.

(12) Papers discussing the principles of Fourier transform ion cyclotron resonance mass spectrometry include: (a) Comisarow, M. B.; Marshall, A. G. *Chem. Phys. Lett.* **1974**, *25*, 282. (b) Comisarow, M. B.; Marshall, A. G. *Chem. Phys. Lett.* **1974**, *26*, 489. (c) Johlman, C. L.; White, R. L.; Wilkins, C. L. *Mass Spectrom. Rev.* **1983**, *2*, 389. (d) Gross, M. L.; Rempel, D. L. *Science* **1984**, *226*, 261. (e) Marshall, A. G. *Acc. Chem. Res.* **1985**, *18*, 316. (f) Russell, D. H. *Mass Spectrom. Rev.* **1986**, *5*, 167.

(13) (a) Buckner, S. W.; VanOrden, S. L. *Organometallics* **1990**, *9*, 1093. (b) VanOrden, S. L.; Pope, R. M.; Buckner, S. W. *Organometallics* **1991**, *10*, 1089.

(14) Comisarow, M. B.; Parisod, G.; Grassi, V. *Chem. Phys. Lett.* **1978**, *57*, 413.

(15) Cody, R. B.; Burnier, R. C.; Reents, W. D.; Carlin, T. J.; McCrery, D. A.; Lengel, R. K.; Freiser, B. S. *Int. J. Mass Spectrom. Ion Phys.* **1980**, *33*, 37.

(16) Pope, R. M.; Cooper, B. T.; VanOrden, S. L.; Buckner, S. W. Manuscript in preparation.

Scheme II

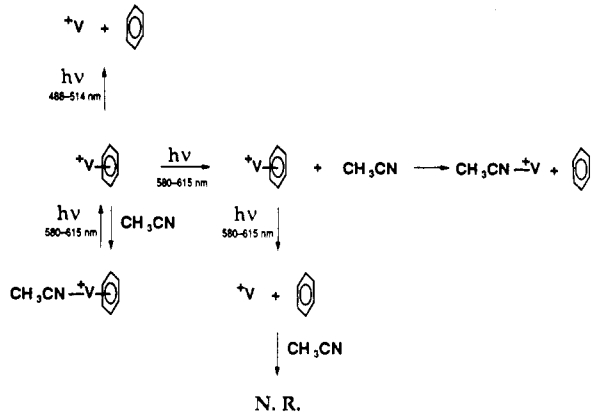

pumped away in ~500 ms. Pressures are monitored with a Granville-Phillips 271 ionization gauge. After 500 ms the $V(C_6H_6)_n^+$ (n = 1, 2) species are isolated prior to photoexcitation and further reaction using swept RF ejection pulses.[14] CH_3CN, butadiene, and NH_3 used for the ligand-switching reactions are admitted into the reaction chamber via Varian variable-leak valves. Typical background pressures of ~(2–6) × 10^{-6} Torr are maintained. All ligands were obtained commercially and used as supplied, except for multiple freeze–pump–thaw cycles to remove noncondensible gases from CH_3CN.

The trapped metal ion complexes are photoexcited with light from a Coherent CW Ar^+/dye laser system. The light pulses are gated with a shutter controlled by a Uniblitz driver. Output from both the Ar^+ laser (all lines ~4 W) and the dye laser (Rhodamine-6G, ~0.5 W peak power, 585–615 nm) is expanded to a 0.75-in. diameter at the cell. The output from the Ar^+ laser is not line-selected and includes primarily 488 and 514 nm. Wavelengths for the dye output are measured using a Burleigh wavemeter. Photodissociation power dependencies were measured by trapping the appropriate complexes in the laser beam for 0–4 s. Photochemically driven reactions were monitored for 0–2 s with continuous irradiation.

Results and Discussion

There is an extensive body of literature on condensed-phase photoinitited ligand substitution reactions proceeding by dissociative mechanisms.[1-3] It is not surprising then to find gas-phase ligand photosubstitution occurring by a dissociative mechanism. However, no examples have been previously reported. Such a dissociative mechanism is observed in the reaction of gas-phase $V(C_6H_6)_2^+$. The photochemical processes for $V(C_6H_6)_2^+$ are shown in Scheme I. Mass spectra for the isolated $V(C_6H_6)_2^+$ in an acetonitrile bath with and without laser irradiation are shown in Figure 1. $V(C_6H_6)_2^+$ is photodissociated to generate an unsaturated $V(C_6H_6)^+$, which slowly attaches CH_3CN to produce $V(C_6H_6)(CH_3CN)^+$. This reaction effectively corresponds to displacement of C_6H_6 in $V(C_6H_6)_2^+$ by CH_3CN—a reaction which does not occur without photoexcitation. A peak corresponding to the oxo–vanadium–benzene ionic complex is also observed upon irradiation. This is due to reaction of the vanadium–benzene complex with a small amount of background oxygen.

A more interesting situation occurs for the reaction of photoexcited $V(C_6H_6)^+$ with CH_3CN. The photochemical processes for this ion are shown in Scheme II. $V(C_6H_6)^+$ absorbs light in the 585–615-nm range and dissociates by a two-photon process. Plots of the power dependence of the photodissociation of $V(C_6H_6)^+$ using 604-nm light and using the output of the Ar^+ laser are shown in Figure 2. If $V(C_6H_6)^+$ collides with background CH_3CN after absorption of one photon (585–615 nm) but prior to absorption of a second photon, ligand switching can occur to generate $V(CH_3CN)^+$. Two experiments were performed

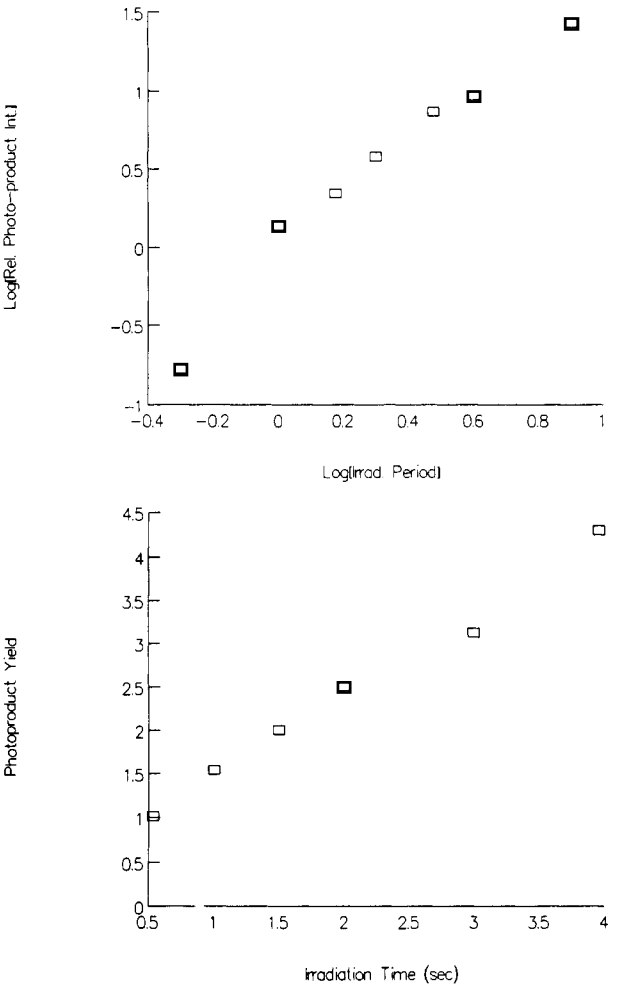

Figure 2. Photoproduct intensity for the photodissociation of $V(C_6H_6)^+$ to generate V^+ and benzene as a function of incident laser power: (a, top) power dependence for dissociation with 604-nm light; (b, bottom) power dependence using the output from an Ar^+ laser.

in order to verify that $V(CH_3CN)^+$ was generated by the associative mechanism shown in Scheme II. To eliminate the possibility of a dissociative mechanism, V^+ was continuously ejected during the photoexcitation event using an RF pulse resonant with m/e 51. This had no effect on the abundance of the $V(CH_3CN)^+$ product. The absence of a dissociative pathway is also substantiated by the observation that V^+, generated directly by laser desorption, does not react with a bath of CH_3CN at a pressure of ~5 × 10^{-6} Torr and reaction times up to 4 s. In a second experiment, the total adduct $V(C_6H_6)(CH_3CN)^+$, which is formed during the trapping (photoexcitation) period, was continuously ejected by an RF ejection pulse. This had no effect on the intensity of the $V(CH_3CN)^+$ product, indicating photodissociation of the adduct does not generate this ion. As a further test, $V(C_6H_6)(CH_3CN)^+$ was formed and isolated by swept double resonance ejection pulses. When the isolated complex was irradiated with 585–615-nm light, dissociation occurred exclusively to form $V(C_6H_6)^+$ (reaction 5).

$$V(C_6H_6)(CH_3CN)^+ + h\nu\ (585\text{–}615\ \text{nm}) \rightarrow V(C_6H_6)^+ + CH_3CN \quad (5)$$

The mechanism for the associative ligand switching reaction shown in Scheme II can be best understood by reference to a simplified potential surface for the reaction, shown in Figure 3. At thermal energies, CH_3CN does not displace benzene from $V(C_6H_6)^+$ ($k^{II} < 10^{-13}$ cm^3/(mol s))

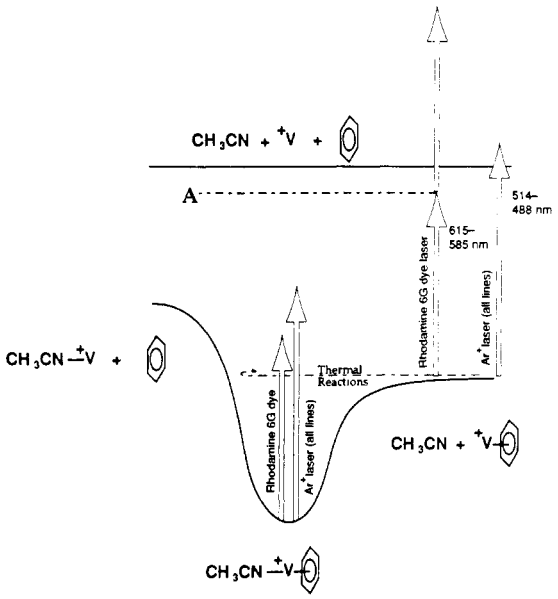

Figure 3. Potential energy diagram for the photoinduced V-$(C_6H_6)^+$ + CH_3CN reaction.

because the reaction is endothermic. The adduct, V-$(CH_3CN)(C_6H_6)^+$, does form slowly by collisional and/or radiative stabilization. $V(C_6H_6)(CH_3CN)^+$ undergoes photodissociation with output from the Ar^+ laser via two channels (reactions 6 and 7). The loss of acetonitrile is

$$V(C_6H_6)(CH_3CN)^+ + h\nu\ (488, 514\ nm) \rightarrow \begin{cases} V(C_6H_6)^+ + CH_3CN & (6)\ 80\% \\ V(CH_3CN)^+ + C_6H_6 & (7)\ 20\% \end{cases}$$

the main pathway due to its lower activation energy. Photoexcitation of $V(C_6H_6)(CH_3CN)^+$ with 585–615-nm light results in exclusive loss of CH_3CN, as previously stated. This is because the activation energy for benzene loss is greater than the photon energy (46–48 kcal/mol). Initial photoexcitation of trapped $V(C_6H_6)^+$ generates an excited ion (~47 kcal/mol internal excitation), which undergoes interconversion to a vibrationally excited level of the ground electronic state. In the low-density environment of the ICR trap, this ion can relax by sequential infrared fluorescence or collisional quenching.[17] Absorption of a second photon induces dissociation to form V^+. However, if the vibrationally excited ion collides with CH_3CN, a highly excited $V(C_6H_6)(CH_3CN)^+$ complex is formed. This ion has internal energy equal to the photoexcitation energy plus the energy of coordination of acetonitrile to $V(C_6H_6)^+$ (internal energy A in Figure 3).

The highly excited $V(C_6H_6)(CH_3CN)^+$ can then partition between the benzene- and acetonitrile-loss pathways. The benzene-loss pathway effectively results in an associative ligand displacement.

The power dependencies for photodissociation allow limits to be placed on the corresponding bond dissociation energies. $V(C_6H_6)^+$ one-photon dissociation is observed with output from the Ar^+ laser and two-photon dissociation is observed at 604 nm (47.2 kcal/mol), implying 68 kcal/mol > $D(V^+–C_6H_6)$ > 57 kcal/mol. For $V(C_6H_6)(CH_3CN)^+$ one-photon dissociation to lose benzene is observed with (488, 514 nm) light and exclusive loss of CH_3CN occurs at 615 nm, indicating 74 kcal/mol > $D((CH_3CN)V^+–C_6H_6)$ > 62 kcal/mol. These results can be compared with a recently reported value of 83 kcal/mol > $D((C_6H_6)V^+–C_6H_6)$ > 75 kcal/mol.[7] This suggests there are not any large cooperative effects in the benzene binding in these complexes.

An attempt was made to induce ligand switching with other ligands, including NH_3 and alkenes. However, the high reactivity of the thermalized $V(C_6H_6)^+$ precluded this. For example, $V(C_6H_6)^+$ reacts with NH_3 to form the imido–vanadium–benzene complex (reaction 8). Irradiation

$$V(C_6H_6)^+ + NH_3 \rightarrow VNH(C_6H_6)^+ + H_2 \quad (8)$$

of $V(C_6H_6)^+$ during the reaction period has no noticeable effect on the product intensity. Reaction of $V(C_6H_6)^+$ with butadiene generates three products (reactions 9–11).

$$V(C_6H_6)^+ + C_4H_6 \rightarrow \begin{cases} V(C_6H_6)(C_4H_6)^+ & (9) \\ V(C_6H_6)(C_4H_4)^+ + H_2 & (10) \\ V(C_6H_6)(C_2H_2)^+ + C_2H_4 & (11) \end{cases}$$

Irradiation produces an enhancement of the product from reaction 10. However, irradiation of the isolated benzene–butadiene–vanadium complex produced in reaction 9 results in loss of H_2. Thus, the enhancement of reaction 10 is most likely due to subsequent dissociation of V-$(C_6H_6)(C_4H_6)^+$ formed during the trapping and irradiation period.

The present results demonstrate photochemical enhancement of gas-phase ligand-switching reactions occurring by both dissociative and associative mechanisms. We have also recently observed photoinduced oxidation and electron-transfer reactions.[18] This work suggests bimolecular gas-phase ion photochemistry will be an interesting field of study which can yield insight into the mechanistic and dynamic aspects of gas-phase organometallic chemistry.

Acknowledgment is made to the donors of the Petroleum Research Fund, administered by the American Chemical Society, for partial support of this work.

OM9105987

(17) (a) Dunbar, R. C. *J. Phys. Chem.* **1983**, *87*, 3105. (b) Hanovich, J. P.; Dunbar, R. C.; Lehman, T. *J. Phys. Chem.* **1985**, *89*, 2513. (c) Dunbar, R. C.; Chen, J.-H.; So, H. Y.; Asomoto, B. *J. Chem. Phys.* **1987**, *86*, 2081. (d) Kim, M. S.; Dunbar, R. C. *Chem. Phys. Lett.* **1979**, *60*, 247.

(18) Cooper, B. T.; Buckner, S. W. Manuscript in preparation.